Physical Communication 35 (2019) 100721

Contents lists available at ScienceDirect

Physical Communication

journal homepage: www.elsevier.com/locate/phycom

Full length article

UAV positioning for out-of-band integrated access and backhaul millimeter wave network☆

Mai A. Abdel-Malek [a,*], Ahmed S. Ibrahim [a], Mohamed Mokhtar [b], Kemal Akkaya [a]

[a] Department of Electrical and Computer Engineering, Florida International University, Miami, 33174, USA
[b] Interdigital Inc., Conshohocken, Philadelphia, 19428, USA

ARTICLE INFO

Article history:
Received 6 September 2018
Received in revised form 10 May 2019
Accepted 21 May 2019
Available online 4 June 2019

Keywords:
3-D positioning
Connectivity
Fiedler value
Integrated access and backhaul network
Millimeter wave
Semi-definite programming
Unmanned aerial vehicle

ABSTRACT

Unmanned Aerial Vehicles (UAVs) can play a major role in enhancing both the access and backhaul networks of the next generation of mobile networks. In this paper, we propose a novel positioning scheme that finds the optimum 3-dimensional flying locations for the UAVs to enhance the connectivity of the backhaul network, while providing the desired quality of service (QoS) for the served users in the access network. The backhaul network connectivity is represented by the algebraic connectivity (or Fiedler value), while the user equipments (UEs) signal reception quality is represented by the signal-to-interference-and-noise-ratio (SINR). We consider an out-of-band integrated access and backhaul (IAB) network, in which we consider the interference that is generated from the deployed UAVs within the access network. The formulated UAV positioning problem is modeled as a low-complexity semi-definite programming (SDP) optimization problem, which can be solved numerically with low complexity. We also consider the access network to experience the propagation modeling of millimeter wave (mm-wave) frequency band. Finally, computer simulations are conducted to show the improvement of the proposed algorithm, in terms of the backhaul algebraic connectivity, while guaranteeing the desired SINR threshold for all the UEs in the access network.

© 2019 Published by Elsevier B.V.

1. Introduction

Nowadays, the utilization of flying Unmanned Aerial Vehicles (UAVs), or drones, in various situations is receiving much attention [1]. For example, in the case of rapid disaster relief [2–6], with the destruction of some of the fixed base stations, UAVs can play a major two-fold role. On one hand, it can *reconnect* the disconnected backhaul network, by acting as *flying multi-hop relays* among the operating base stations. On the other hand, UAVs can provide *coverage* to the disconnected user equipments (UEs). Towards jointly achieving both goals, the UAVs locations need to achieve a good balance between the connectivity of the backhaul network along with the coverage of the access network. In other words, there is a need for finding the best locations of the UAVs deployed for an integrated access and backhaul (IAB) network.

The next generation of mobile networks (NGMN), including 5G system and beyond, need to provide high data rate as one of its fundamental requirements. UAV-based NGMN can contribute to such high data rate via utilizing the wide-bandwidth millimeter wave (mm-wave) frequency band [7–10]. Such high data rate objective requires a full functional links, which is of great importance to the UAV-based communication given their short lifetime due to their battery-operated mode.

There have been recent works focusing on 3-dimensional (3-D) UAV positioning to serve multiple purposes either to increase the connectivity of the backhaul network [11–13], or to increase the coverage of the served UEs [14–17]. First, we focus on optimizing the UAVs positions to only enhance the *coverage*. In [18], the authors derived a closed-form expression for the UAV position to maximize the coverage radius in the presence of Rician fading model. Optimal UAV positioning schemes to enhance the outage probability or signal-to-interference-and-noise-ratio (SINR), were discussed in [14,15], respectively. In terms of achieving specific user data rates, a 3-D positioning of UAVs is investigated in [17], with users having different rate requirements for urban networks. Furthermore, the utilization of a UAV in device-to-device (D2D) communication was considered in [16], in which the UAV acts as a flying base station in a network of users engaged in the D2D communication.

Second, the UAV positioning has been also considered for *connectivity* enhancement. For example, steering UAV for off-shore network recovery and rare territories with poor network

☆ The work of M.A. Abdel-Malek and A.S. Ibrahim is supported in part by the National Science Foundation under Award No. CNS-1618692.

* Corresponding author.
E-mail addresses: mabde030@fiu.edu (M.A. Abdel-Malek), aibrahim@fiu.edu (A.S. Ibrahim), mohamed.awadin@interdigital.com (M. Mokhtar), kakkaya@fiu.edu (K. Akkaya).

https://doi.org/10.1016/j.phycom.2019.100721
1874-4907/© 2019 Published by Elsevier B.V.

construction was considered in [11] to improve the network connectivity. Utilizing the UAV to enhance the connectivity was proposed in [12], in which the authors derived the probability of an arbitrary node being isolated as a representation of the network connectivity. In [13], a coverage-based and a connectivity-based mobility models were introduced towards a UAV network monitoring. A comparison between both models is conducted to clarify the tradeoff between achievable area coverage for the connectivity-based model and achievable connectivity for the coverage-based model. It is worth mentioning that in [13] both models were considered *separately*, unlike this paper in which we propose an integrated solution that considers both coverage and connectivity *simultaneously*.

Furthermore, the *mm-wave* communication has recently received great attention in terms of its channel measurements, modeling, and system design. For example In [19], the authors built an indoor communicating system to test and measure the mm-wave 60 GHz propagation patterns, and they introduced a statistical model for indoor multipath propagation. The ergodic capacity of an outdoor clustered mm-wave network with directional antennas is proposed in [20], which utilizes the directional beamforming and uncoordinated channel access in order to provide cluster capacity gains. UAV positioning has been previously considered in mm-wave band as well [21]. For example, an autonomous relay scheme was proposed in [22], and it uses mobile relays to extend the coverage of the mm-wave communication. However and unlike the work of this paper, there has been no consideration of the network connectivity measures.

We point out that none of the aforementioned works optimized the UAV position to *jointly* extend the access network coverage and enhance the backhaul network connectivity. To the best of our knowledge, this work is the first to address the tradeoff between coverage and connectivity, and how to improve such tradeoff through the utilization and optimization of UAVs positioning.

In this paper, we aim to find the optimum locations for a set of UAVs, operating in the mm-wave frequency band, to achieve a good coverage–connectivity tradeoff in an IAB mm-wave network. On one hand, the network connectivity is characterized in terms of the algebraic connectivity (Fiedler value) [23,24], which is the second smallest eigenvalue of the Laplacian matrix representing the backhaul network graph. On the other hand, the coverage is defined by the threshold on the SINR. We consider an out-of-band (OOB) IAB network, in which there is no interference between the access and backhaul networks, as they operate on different frequency band. However, interference within the access network is considered and mitigated by optimizing the UAV's locations. Given such system and considerations, we formulate the UAV optimization problem as finding the optimal UAVs locations that maximize the backhaul network connectivity, while maintaining the desired the formulated UAV-based OOB IAB problem, we relax it through a number of steps to be formulated as a low-complexity semi-definite programming (SDP) optimization problem. Computer simulations are conducted taking into consideration the relevant mm-wave frequency ranges and channel models. The results of the proposed schemes show higher connectivity measures (Fiedler value), while achieving the desired SINR threshold for UEs.

Our contributions in this paper can be summarized as follows:

- Formulating a novel UAV-based IAB positioning problem, in which we aim to maximize the *backhaul* network connectivity, while providing the desired SINR for all users in the *access* network.
- Mathematically relaxing the formulated optimization problem to be an SDP one, which can be solved numerically with reasonable complexity.
- The proposed algorithm finds the best positions for the considered UAVs, enhances the algebraic connectivity of the backhaul network for various number of UAVs, and achieves the desired SINR for all the user over the mm-wave access network.

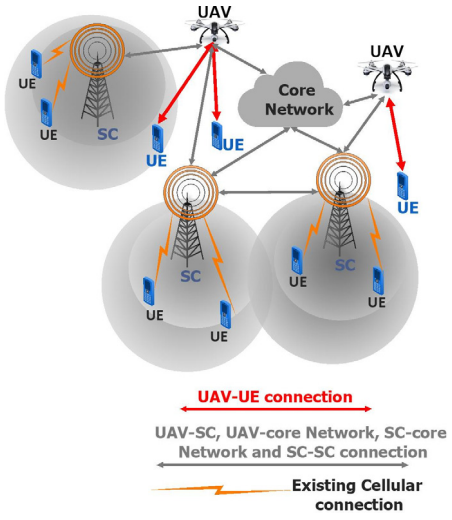

Fig. 1. System model of UAV-based integrated access and backhaul network.

We point out that in our previous work [25], we have presented the initial results of this work in which we only considered a *single* UAV to enhance the backhaul connectivity while improving the coverage of UEs. In this paper, we extend our initial work in [25] to the case of multiple UAVs in which we also aim to mitigate the undesired interference generated from the UAVs.

The rest of the paper is organized as follows, first the system model describing both the access and backhaul networks is described in Section 2. The optimization problem is formulated in Section 3. Section 4 introduces the problem relaxation and the proposed solution. Finally, numerical results and concluding remarks are provided in Sections 5 and 6, respectively.

Notation: Lower- and upper-case bold letters denote vectors and matrices, respectively, also $\mathbf{I}_M$ denotes the identity matrix of size M. The operations $(\cdot)^T$, $\mathbb{E}[\cdot]$, and $|\cdot|$ denote the transpose, statistical expectation and absolute value, respectively. The $\mathbf{A} \preceq \mathbf{B}$ denotes that $\mathbf{B} - \mathbf{A}$ is a positive semi-definite matrix. Finally, $\otimes$ denotes the Kronecker product operation.

2. System model

In this section, we describe the system model covering both the access and backhaul networks. Fig. 1 depicts an IAB network which generally consists of N Small Cells (SC) and M UEs. The N SCs are generally connected with each other as well as with the core network. Some of the UEs are served by their closest SCs over mm-wave frequency band, while other UEs are outside the coverage area of all the SCs. In Fig. 1, we show that a UAV can be deployed to serve two purposes. First, it can enhance the connectivity of the backhaul network by relaying information among the SCs and core network. Second, it can serve the UEs who are initially out of the SCs coverage.

We consider an out-of band (OOB) IAB network, where the transmissions from the UAVs to SCs and UEs are assumed to be

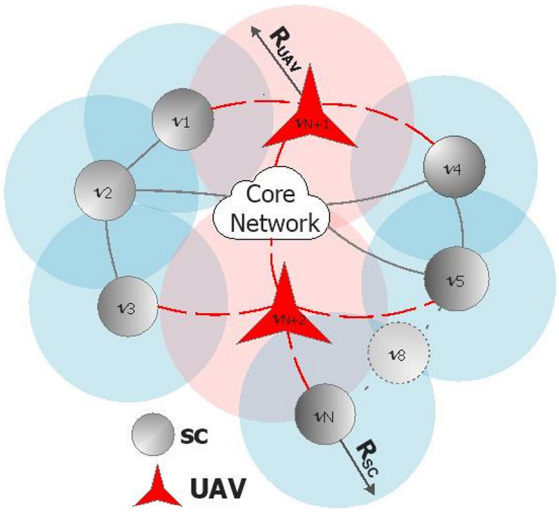

Fig. 2. Backhaul network modeling.

frequency division multiplexed (FDM), i.e., UAV-to-SC and UAV-to-UE communication links occur over different carrier frequencies with no interference between these two tiers. In the next subsections, we introduce how to utilize graph theory in modeling the backhaul network, while modeling the access network using communication theory.

2.1. Graph-theoretic backhaul network modeling

The field of *graph theory* provides a good mathematical framework to analyze the connectivity of the backhaul network. Therefore in this paper, we consider a graph-theoretic approach to model the backhaul network of small cells and UAVs as follows. Fig. 2 depicts the modeling of the SC backhaul network as an undirected weighted finite graph $\mathcal{G}(\mathbf{V}, \mathbf{E})$ where $\mathbf{V} = \{v_1, v_2, \ldots, v_N\}$ is the set of the SCs nodes and $\mathbf{E} = \{e_1, e_2, \ldots, e_Q\}$ is the set of all Q edges (links) among the SCs. The undirected graph implies that all the links in the network are bidirectional. Edges are defined based on the distance-based disk model [26]. In the considered disk model, an edge exists between two nodes if the distance between those nodes is less than R_{SC}. We point out that the orthogonal transmission among the SCs and UAVs results in no interference, and hence it is accurately represented by the distance-based model.

For an edge q, $1 \leq q \leq Q$, connecting nodes $v_i, v_j \in V$, define the edge vector $\mathbf{a}_q \in \mathbf{R}^{N\times 1}$, where the i^{th} and j^{th} elements are given by $a_{q,i} = 1$ and $a_{q,j} = 1$, respectively, and the rest is zero. The relationship between the N vertices and the corresponding Q links between those vertices in $\mathcal{G}$ is captured in a matrix named the incidence matrix $\mathbf{A} \in \mathbf{R}^{N\times Q}$, where the q^{th} column is given by $\mathbf{a}_q$. For this undirected graph, the Laplacian matrix $\mathbf{L}(\mathbf{A}) \in \mathbf{R}^{N\times N}$ is defined as:

$$\mathbf{L}(\mathbf{A}) = \mathbf{A}\,\mathrm{diag}(\mathbf{w})\mathbf{A}^T = \sum_{q=1}^{Q} w_q \mathbf{a}_q \mathbf{a}_q^T, \tag{1}$$

where $\mathbf{w}$ denotes the $q \times 1$ weighting vector coefficients for the q edges and is given by $[w_1, w_2, \ldots, w_q]^T$ and $\mathrm{diag}(\mathbf{w})$ is $Q \times Q$ diagonal matrix with the $\mathbf{w}$ as the diagonal elements. The Laplacian matrix for such graph is positive semi-definite, which is expressed as $\mathbf{L}(\mathbf{A}) \succcurlyeq 0$ and also its smallest eigenvalue is zero, i.e., $\lambda_1(\mathbf{L}(\mathbf{A})) = 0$. The second smallest eigenvalue of $\mathbf{L}(\mathbf{A})$, $\lambda_2(\mathbf{L}(\mathbf{A}))$, is the algebraic connectivity, or Fiedler value, of the graph $\mathcal{G}$ [27,28]. In this paper, the Fiedler value will be utilized to measure the backhaul network connectivity.

Furthermore, with the UAVs deployment, a new graph $\mathcal{G}'$ is obtained with the same number of N nodes, with a larger set of edges denoted by $\mathbf{E}'$ with Q' edges where $Q' \geq Q$, i.e., $\mathbf{E} \subseteq \mathbf{E}'$, thanks to the UAVs for connecting the SCs within its disc radius R_{UAV}. Particularly, the UAV's impact appears in relaying information between SCs within a distance of R_{UAV}, hence creating additional $Q' - Q$ edges between the original SCs. The potential impact of the UAV deployment over the network connectivity can be quantified by computing the difference $\lambda_2(\mathbf{L}(\mathbf{E}')) - \lambda_2(\mathbf{L}(\mathbf{E}))$.

2.2. Interference-based access network modeling

In this section, we introduce the modeling of the downlink access network which consists of small cells or UAVs on one side and UEs on the other side. Our goal is to model the received SINR at UEs, which is the main QoS metric for UEs. To calculate the SINR, we assume a distance-based association model in which each UE will be served by its closest serving station, which is either an SC or a UAV. Moreover, K_J UAVs are jointly assigned to serve the UEs and SCs. The remaining $K - K_J$ UAVs are only used to enhance the SCs connectivity. In addition to the conventional association model, we also consider a *load balancing* scheme to have equal share of users assigned to each serving station. More precisely, the UAVs serving the UEs are selected depending on their distance from each UAV with an equal UEs distribution for each UAV. The maximum number of UEs, attached to each UAV, is equal to $\frac{M}{K_J}$.

Along with the considered distance-based association model, we also take into considering multiple interference sources as follows. The interference-based model is shown in Fig. 3, where the received signal at any UE is the desired signal from the assigned UAV along with additional interfering signals. There are two different interference sources, as shown in Fig. 3. One is the interference from the same UAV assigned to the user while serving other assigned users. The second source of interference is from other UAVs that are serving their assigned users.

The received signal at a given UE, i, which is associated with the k^{th} UAV can be modeled as

$$y_i = \sqrt{P_{k,UE}}\; h_{k,i}\, d_{k,i}^{-\alpha/2} x_{k,i} + I_i + n_i, \tag{2}$$

where $P_{k,UE}$ is the transmitted power from the k^{th} UAV. We assume equal power distribution among all UEs assigned to the k^{th} UAV. The $h_{k,i}$ is the channel coefficient corresponding to the channel between the k^{th} UAV and the i^{th} UE. Furthermore, $x_{k,i}$ represents the transmitted symbol from the k^{th} UAV towards its potentially-served i^{th} UE with a unit power $\mathbb{E}\{|x_{k,i}|^2\} = 1$ and $d_{k,i}$ denotes the distance between the k^{th} UAV and the i^{th} UE. n_i denotes complex zero-mean circularly-symmetric additive white Gaussian noise (AWGN) with variance σ^2, representing the noise at the i^{th} UE, and it is assumed to be independent across the UEs. Moreover, I_i represents the interference for the i^{th} UE, where

$$I_i = \sum_{m=1, m\neq i}^{M/K_J} \sqrt{P_{k,UE}}\; h_{k,i} d_{k,i}^{-\alpha/2} x_{k,m} + \sum_{j=1, j\neq k}^{K_J} \sum_{m=1}^{M/K_J} \sqrt{P_{j,UE}}\; h_{j,i} d_{j,i}^{-\alpha/2} x_{j,m}, \tag{3}$$

where $P_{j,UE}$ is the transmitted power from the j^{th} UAV to other users.

As previously shown in Fig. 3, deploying multiple UAVs simultaneously introduces two type of interference. The first interference is due to the users served by the same UAV which is the first part of I_i. The second type of interference is due to signals from other UAVs.

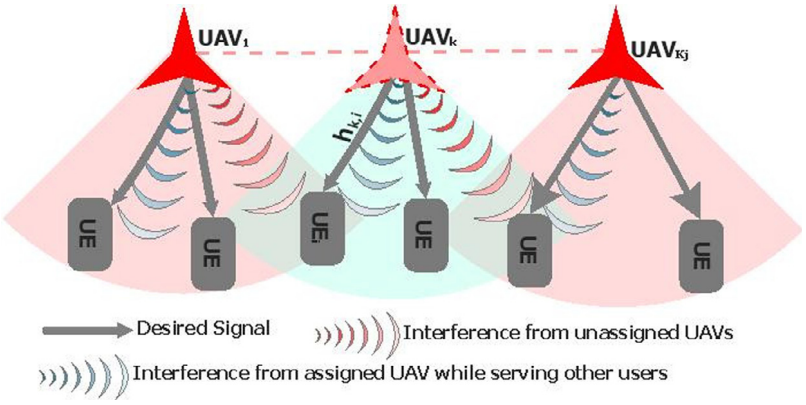

Fig. 3. Interference-based access network modeling.

Then, the SINR of all the UEs is given by $\boldsymbol{\gamma} \in \mathbf{R}^{M\times 1}$, where each element represents the i^{th} UE SINR and is given by

$$\gamma_i = \frac{P_{k,UE}\ d_{k,i}^{-\alpha}\ \left|h_{k,i}\right|^2}{P_{l_i} + \sigma^2}. \tag{4}$$

where P_{l_i} is the interference power given as

$$P_{l_i} = \sum_{m=1,m\neq i}^{M/K_J} P_{k,UE}\ d_{k,i}^{-\alpha} + \sum_{j=1,j\neq k}^{K_J}\sum_{m=1}^{M/K_J} P_{j,UE}\ d_{j,i}^{-\alpha}. \tag{5}$$

For large network of multiple SCs and UAVs, we can assume that we will have large number of small terms representing the interference in Eq. (3). Therefore and for simplicity of analysis and making use of the central limit theory, their addition can be represented by their average value. In other words, we can ignore the small-scale channel coefficients in the interference term Eq. (3), while calculating the interference power in Eq. (5). Therefore, the interference term in Eq. (3) depends only on large scale fading.

3. Problem formulation

In this section, we formulate the UAV-based IAB positioning problem, in which we aim to maximize the backhaul network connectivity, while providing the desired SINR for all users in the access network. For the backhaul network with K UAV deployment, a new graph $\mathcal{G}'$ is obtained with the same number of N nodes, a larger set of edges denoted by $\mathbf{E}'$ with Q' edges where $Q' \geq Q$, i.e., $\mathbf{E} \subseteq \mathbf{E}'$. As was shown previously in Fig. 2, a given UAV can create a new edge between two SCs, if they fall within its communication range, by relaying the information among them. Then, the optimization problem of deploying K UAVs to increase the backhaul connectivity, while providing the desired SINR to the UEs, is formulated as

$$\begin{aligned} &\max_{\mathbf{E}'} \quad \lambda_2(\mathbf{L}(\mathbf{E}')) \\ &\text{s. t.} \quad \gamma_i \geq \gamma_{\text{th}},\ \forall i \in \{1,\ \ldots,\ N\}, \\ &\qquad M\ \ P_{k,UE} + n\ \ P_{k,SC}\ \ \leq P_{UAV},\ \forall k \in \{1,\ \ldots,\ K_J\}, \\ &\qquad (N-n)\ \ P_{k,SC}\ \ \leq P_{UAV},\ \forall k \in \{K_J+1,\ \ldots,\ K\}, \end{aligned} \tag{6}$$

where $P_{k,SC}$ is the transmission power from the k^{th} UAV to a single SC and P_{UAV} is the UAV maximum transmission power, we assume all the UAVs have the same maximum transmission power. Also, n is the number of SCs which the UAVs serve jointly with UEs and $(N-n)$ is the remaining SCs which are served separately by the extra UAVs.

The objective function is to maximize the SCs backhaul connectivity represented by the algebraic connectivity (Fiedler value), introduced in Section 2.1. Then, three constraints are considered: the first constraint is to provide a QoS to the UEs by assuring a certain SINR level to each UE. The next two constraints are to ensure that the maximum UAV power is not violated by either the SCs or the UEs connections. We assume the UAV power is equally distributed between the UAV-SC and UAV-UE connections. Also, the total power allocated to the UAV-UE links is equally distributed over all UEs assigned to the UAV, and similarly the total power allocated to the UAV-SC is equally allocated to all SCs. The total UAV power, P_{UAV}, is equally divided into two groups, namely, the group of UEs and the group of SCs. Half of the UAV power, $\frac{P_{UAV}}{2}$, is equally divided among the transmissions to all the UEs associated with the UAV. The second half of the UAV power, $\frac{P_{UAV}}{2}$, is equally divided among the transmissions towards all the SCs connected with the UAV.

4. Problem relaxation and proposed solution

In the next section, we introduce the proposed approach on how to relax the optimization problem under consideration, then present the proposed solution.

4.1. Problem relaxation

Since each UAV can be deployed anywhere in the 3-D network, the location of each UAV is considered as a continuous variable, which belongs to the interval $([0, h], [0, h], [0, h])$. It has been shown that this problem is NP-hard in [29]. To tackle this NP-hard problem [30], we convert the continuous optimization problem into a discrete one by considering that the SCs and UEs are distributed over $h\times h\times h$ volume. Moreover, the search space over the x, y, and z axes is uniformly quantized with a step size δ to get a search grid consisting of β candidate positions for the UAV, which converts the continuous deploying to a discrete search in a finite number of available positions on the grid.

Thus, the Laplacian matrix is represented by the following formula:

$$\mathbf{L}(\mathbf{E}') = \mathbf{L}(\mathbf{E}) + \sum_{j=1}^{\beta} x_j \mathbf{A}_j\, \text{diag}(\mathbf{w}_j)\mathbf{A}_j^T, \tag{7}$$

where $\mathbf{L}(\mathbf{E})$ is the original graph before UAV deployment and $x_j = 1$ if UAV is positioned in the j^{th} grid point, otherwise $x_j = 0$. Moreover, $\mathbf{w}_j$ and $\mathbf{A}_j$ are the weighting coefficients vectors and the incidence matrix when the UAV is deployed in this grid point. Collecting $x_j,\ j \in \{1,\ \ldots,\ \beta\}$, in the $\beta \times 1$ vector $\mathbf{x}$, Eq. (7) can be written as follows:

$$\mathbf{L}(\mathbf{E}'(\mathbf{x})) = \mathbf{L}(\mathbf{E}) + (\mathbf{x} \otimes \mathbf{I}_M)\ \boldsymbol{\Gamma}, \tag{8}$$

where

$$\boldsymbol{\Gamma} \triangleq \left[\left(\mathbf{A}_1 \operatorname{diag}(\mathbf{w}_1)\mathbf{A}_1^T\right)^T, \ \ldots, \ \left(\mathbf{A}_\beta \operatorname{diag}(\mathbf{w}_\beta)\mathbf{A}_\beta^T\right)^T\right]^T. \tag{9}$$

Then the Backhaul connectivity enhancement problem can be formulated as

$$\begin{aligned} \max_{\mathbf{x}} \quad & \lambda_2(\mathbf{L}(\mathbf{A}(\mathbf{x}))) \\ \text{s. t.} \quad & \gamma_i \geq \gamma_{\text{th}}, \ \forall i \in \{1, \ \ldots, \ N\}, \\ & M \ \ P_{k,UE} + n \ \ P_{k,SC} \ \leq P_{UAV}, \ \forall k \in \{1, \ \ldots, \ K_J\}, \\ & (N-n) \ \ P_{k,SC} \ \leq P_{UAV}, \ \forall k \in \{K_J+1, \ \ldots, \ K\}, \end{aligned} \tag{10}$$

where $\mathbf{x} \in \{0, 1\}$.

Furthermore, we accumulate the SINR levels between the i^{th} UE and the associated UAV in a matrix $\mathbf{V} \in \mathbf{R}^{\beta \times M}$ such that each column, $\mathbf{v}_i$, can be written as

$$\mathbf{v}_i = \left[\gamma_i|_{\{d_{k,i},d_{k,j}\}\in\mathbf{D_1}}, \gamma_i|_{\{d_{k,i},d_{k,j}\}\in\mathbf{D_2}}, \ldots, \gamma_i|_{\{d_{k,i},d_{k,j}\}\in\mathbf{D_\beta}}\right]^T, \tag{11}$$

where $\mathbf{D_i} \in \mathbf{R}^{M\times K_J}, \forall i \in \{1, 2, \ldots, \beta\}$ is the distance between each UE and each UAV at only certain positions within the grid points only $(1, 2, \ldots, \beta)$.

Hence, the optimization problem can be written in terms of the UAV position index vector $\mathbf{x}$ as follows

$$\begin{aligned} \max_{\mathbf{x}} \quad & \lambda_2(\mathbf{L}(\mathbf{A}(\mathbf{x}))) \\ \text{s. t.} \quad & \mathbf{x}^T\mathbf{V} \geq \mathbf{1}^T\gamma_{\text{th}}, \\ & \mathbf{1}^T\mathbf{x} \leq K, \ \mathbf{x} \in \{0, 1\}, \\ & M \ \ P_{k,UE} + n \ \ P_{k,SC} \ \leq P_{UAV}, \ \forall k \in \{1, \ \ldots, \ K_J\}, \\ & (N-n) \ \ P_{k,SC} \ \leq P_{UAV}, \ \forall k \in \{K_J+1, \ \ldots, \ K\}, \end{aligned} \tag{12}$$

We relax the constraint on the entries of $\mathbf{x}$ and allow them to take any value in the interval $[0, 1]$. $\lambda_2(\mathbf{L}(\mathbf{A}(\mathbf{x})))$ can be written as the point-wise infimum of a family of linear functions of $\mathbf{x}$ as

$$\lambda_2(\mathbf{L}(\mathbf{A}(\mathbf{x}))) = \inf_y [y^T\mathbf{L}(\mathbf{A}(\mathbf{x}))y, \ \|y\|_2 = 1, \ \mathbf{1}^T y = 0]. \tag{13}$$

Hence, it is a concave function in $\mathbf{x}$. In addition, the relaxed constraints are linear in $\mathbf{x}$. Therefore, the optimization problem is a convex optimization problem with linear constraints. Furthermore, the optimization problem in Eq. (6) can be written as a Semi-definite Programming (SDP), which is a sub category of the convex optimization.

The relaxed SDP optimization problem can be written as follows [31]

$$\begin{aligned} \mathbf{P1}: \max_{\mathbf{x},s} \quad & s \\ \text{s. t.} \quad & s(\mathbf{I} - \frac{1}{\beta}\mathbf{1}\mathbf{1}^T) \preceq \mathbf{L}(\mathbf{A}(\mathbf{x})), \\ & \mathbf{x}^T\mathbf{V} \geq \mathbf{1}^T\gamma_{\text{th}}, \\ & \mathbf{1}^T\mathbf{x} \leq K, \ 0 \leq \mathbf{x} \leq 1, \\ & M \ \ P_{k,UE} + n \ \ P_{k,SC} \ \leq P_{UAV}, \ \forall k \in \{1, \ \ldots, \ K_J\}, \\ & (N-n) \ \ P_{k,SC} \ \leq P_{UAV}, \ \forall k \in \{K_J+1, \ \ldots, \ K\}. \end{aligned} \tag{14}$$

4.2. Proposed solution

The relaxed SDP problem in Eq. (14) can be solved using an *SDP* solver such as CVX SDPT3 solver [32]. Afterwards and since the entries of output vector $\mathbf{x}$ are continuous, we choose the maximum entry and set it to 1, while others are set to zero.

Algorithm 1 summarizes the solution steps as follows, first, the total 3-D area is quantized to the $h \times h \times h$ cubes as mentioned in Section 2. Then, the new network including both the SCs and the UAVs is defined using the incidence matrix $A(x)$ for all the permutations of possible positions (cubes) in the grid, $P(\beta)$. Next, we construct the distance matrix, $\mathbf{D}$, of all possible locations for the UAVs. Also, we construct the association matrix, $\mathbf{S}(\mathbf{D})$, to find the UEs assigned to each UAV depending on the distance matrix and the maximum load assigned to each UAV.

Algorithm 1: *K* UAVs Positioning.

```
Input: (x_SC, y_SC, z_SC) and (x_UE, y_UE, z_UE)
A ← the graph incidence Matrix
λ2(L(A)) ← connectivity of SCs
Quantize:
β ← Grid positions
x ← β × 1 vector
P(β) ← permutation of all grid positions
for ∀k ≤ K_J & ∀P(β) do
Link Matrix:
    A(x) ← Link matrix after adding UAVs
    L(x) ← Laplacian matrix after adding UAVs
Association ∀k ≤ K_J:
    D ← Distance matrix after adding UAVs
    S(D) ← association matrix after adding UAVs
    I(S(D)) ← Interference matrix
    γ(I(S(D)), D) ← The UEs SINR
end for
for K do
Optimization:
    max_x  λ2(L(A(x)))
    if γ(D) ≥ γ_th & UAV total power ≤ P_UAV then
        Break
    else
        goto Optimization.
        (x_UAV, y_UAV, z_UAV) ← max_K(x).
    end if
end for
Output: (x_UAV, y_UAV, z_UAV)
```

Next, the optimization solver is executed to find the maximum backhaul network connectivity , while providing the desired SINR, γ_{th}, for all users in the access network. The output optimized UAVs locations in the grid system is obtained as a probability distribution of $0 \leq \mathbf{x} \leq 1$ due to the SDP relaxation. Hence, We obtain the UAVs locations by finding the maximum K values of $\mathbf{x}$. Then, the UAVs Cartesian locations are calculated by reversing the gridding quantization operation.

In terms of the complexity of the proposed algorithm, first we point out that the interior point algorithms for solving SDP optimization problems are shown to be polynomial in time [33]. Therefore, the proposed UAV positioning scheme which applies a small number of iterations, each requires solving SDP optimization problem, has a polynomial complexity in time.

Finally, we point out that the proposed solution will be implemented via a central node (e.g. core network) that has access to all the information in the network, which are needed to solve the optimization problem in Eq. (14). The central node will accordingly direct the UAVs to take their positions according to the obtained solution.

5. Simulation results

In this section, we present simulation results to demonstrate the achievable performance of the proposed UAV-based IAB positioning algorithm. Our goal is to show the performance improvement in the backhaul network connectivity, while providing the desired SINR for all users in the access network. For comparison purposes, we also consider a *random* positioning approach, in

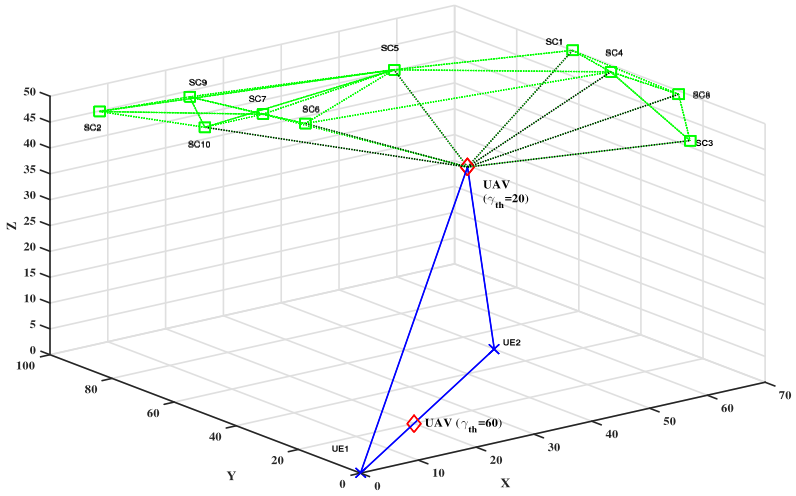

Fig. 4. UAV positioning for different γ_{th}. The square, cross and diamond markers represent SC, UE and UAV, respectively.

Table 1
Simulation parameters.

Parameter	Value
h	100 m
N	10
M	2
K	1
R_{SC}	40 m
R_{UAV}	40 m
α	4
σ^2	−130 dBm
P_{UAV}	30 dBm
δ	6 m
γ_{th}	30 dB

which the UAVs are deployed randomly while the SINR threshold constraints are satisfied for all the UEs. The simulation is executed using MATLAB SDPT3 solver with the simulation parameters listed in Table 1. The results are averaged over 10^3 different backhaul network realizations and UEs deployment locations. Then for the 28 Ghz mm-wave, channel coefficients are obtained through NYUSIM [34], which is a developed channel model simulator for the mm-wave wireless communications.

Next, we present the results for the single UAV deployment in Section 5.1. The multiple UAV simulation results are presented in Section 5.2.

5.1. Single UAV simulation results

In this section, we show the solution of the approximated SDP optimization in Eq. (14) to find the optimal deployment of a single UAV deployment problem. We assume no interference case, and hence, the SINR threshold is treated as only SNR threshold. The impact of changing γ_{th} on the UAV positioning is shown in Fig. 4, where the UAV position in the 3-D search grid with red diamond markers is plotted for two extreme cases for the UEs constraints. In the first case, $\gamma_{th} = 20$ dB corresponding to low QoS constraint. In this case, the UAV gets closer to the SCs to enhance the backhaul network connectivity. The original network connectivity is $\lambda_2(\mathbf{L}(\mathbf{x})) = 2.015$ and the UAV deployment achieves $\lambda_2(\mathbf{L}(\mathbf{x})) = 6.476$, which is more than three times the original backhaul connectivity. In the other case at $\gamma_{th} = 60$ dB, which represents a high QoS constraint, the UAV gets closer to the UEs to satisfy their tight constraints with no improvement for the backhaul network connectivity.

Table 2
Convergence analysis of the SDP algorithm.

SDPT3 status	Percentage
Solved	90%
Failed/Unbounded	10%

5.1.1. Quantization step size

Fig. 5 investigates the performance of the quantizing relaxation as compared to the unquantized optimization problem in Eq. (6). It depicts the Fiedler value of the SCs backhaul network graph, as a function of the UEs SNR threshold γ_{th}. The unquantized optimization is solved using the non-convex *fmincon* numerical solver in MATLAB, with multi-initial point searching to avoid local minima situations. Assuming $\delta = 8$ m in Eq. (14) for the quantized SDP optimization, Fig. 5 shows that increasing the γ_{th} decreases the connectivity for the different schemes. It is shown that the SDP-based quantized solution achieves nearly 35% gain compared to the random positioning scheme, for $\gamma_{th} = 30$ dB. It is also shown the that proposed SDP-algorithm achieves algebraic connectivity of 5.25, while the non-convex solver achieves 6.5. Hence, there is a performance gap of 24% due to relaxing the original non-convex optimization problem in this case.

To reduce the performance gap between the unquantized optimization and the SDP-based solution we decrease the step size to $\delta = 6$ m, which results in a higher quantization resolution. As shown in Fig. 6, the output from the SDP optimization is the same as the unquantized optimization for all values of γ_{th}. Furthermore, at SNR threshold $\gamma_{th} = 30$ dB and considering $\delta = 6$ m, the quantized SDP-based solution achieves gain of 60%, compared to the random positioning scheme. All the simulation results presented in the rest of this paper will be based on quantization step of $\delta = 6$ to avoid any performance gap due to relaxing the original non-convex optimization problem.

5.1.2. Convergence of the proposed SDP-based algorithm

In this subsection, we show the convergence of the proposed solution, which is an integral characteristic of any iterative solution. In implementing the proposed solution, we have utilized the SDPT3 solver. Such solver produces the status of its iterations, once concluded, which can be "solved", "Failed", or "unbounded". In an attempt to characterize the convergence of the proposed iterative solution, we show in Table 2 the ratio of the "solved"

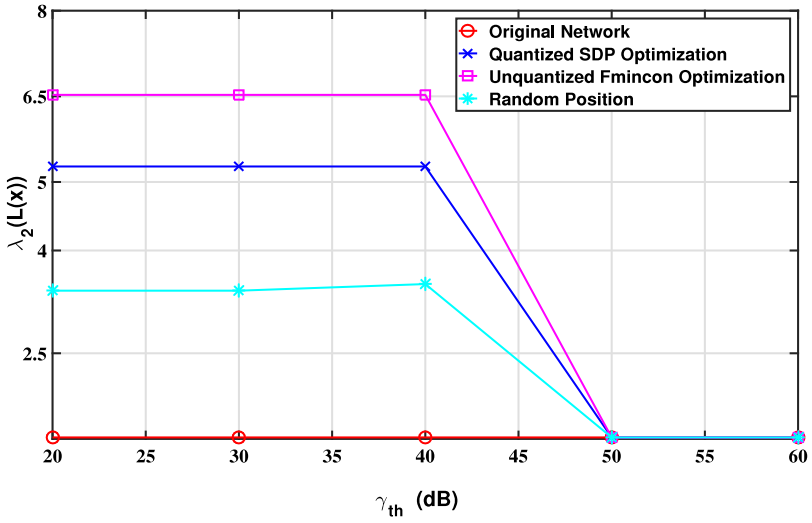

Fig. 5. The connectivity of the SCs versus the UEs SNR constraint for $\beta = 2197$, $\delta \cong 8$ m.

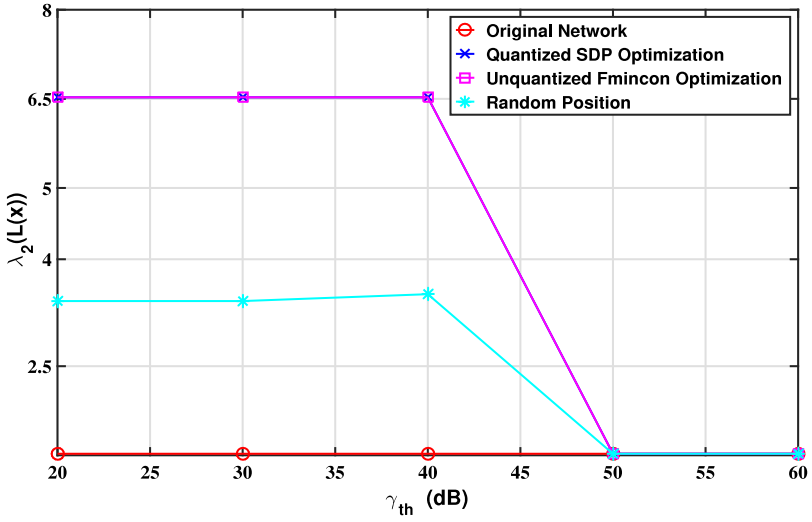

Fig. 6. The SCs connectivity versus the UEs SNR constraint for $\beta = 3,375$, $\delta \cong 6$ m.

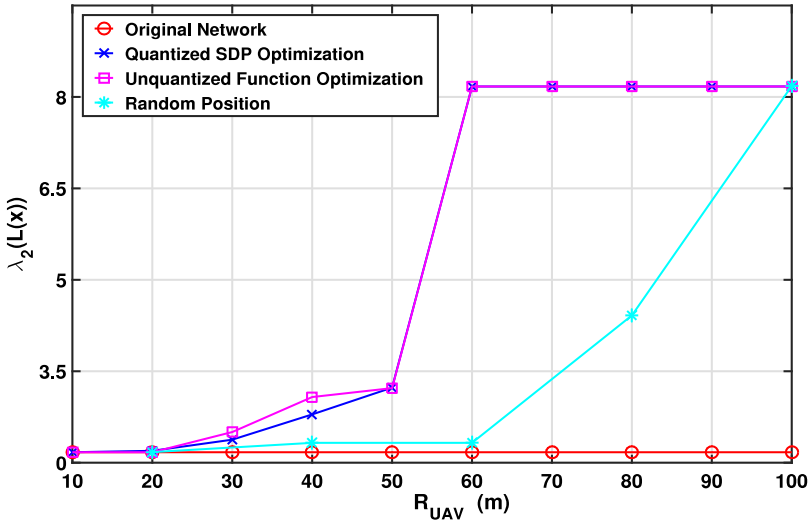

Fig. 7. The SCs connectivity versus the UAV transmission range for $\beta = 3,375$, $\delta \cong 6$ m.

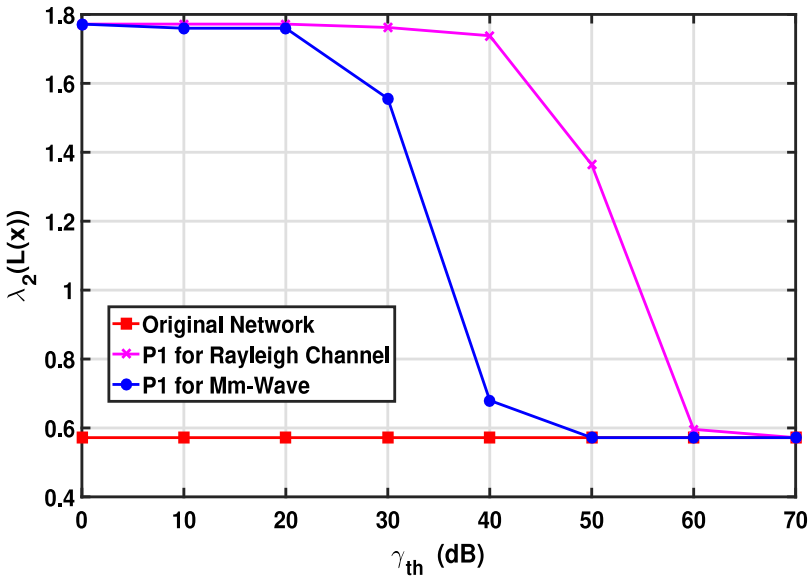

Fig. 8. The Rayleigh fading channel versus the mm-wave channel.

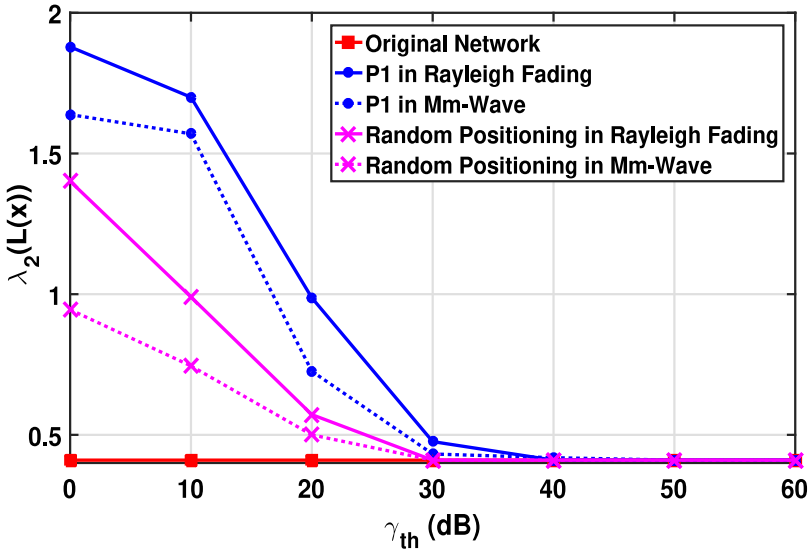

Fig. 9. The connectivity of the SCs versus the UEs γ_{th} for $K = 2$ UAVs.

status, as opposed to the other ones, for 500 different network deployment scenarios. As shown, 90% of the iterations have resulted in a "solved" status leading to an optimum solution.

5.1.3. UAV Transmission range

In this subsection, we investigate the effect of the UAV transmission range on the backhaul connectivity. In Fig. 7 the algebraic connectivity of the SCs backhaul network is plotted against the UAV transmission range, R_{UAV}. As shown, the backhaul connectivity enhances with the increase of the UAV transmission range. As the UAV transmission radius increases beyond a certain threshold, the network algebraic connectivity saturates at its maximum possible value. Similar to the above results, the proposed SDP-based solution outperforms the random positioning scheme.

5.1.4. Millimeter wave channel impact

In this subsection, we will investigate the impact of the mm-wave channel on the connectivity of the SCs backhaul network. The mm-wave channel model at 28 Ghz is obtained through NYUSIM [34]. Fig. 8 depicts the algebraic connectivity considering both the *Rayleigh* and the mm-wave channel fading channel and assuming $\alpha = 4$. As a result of higher-frequency of the mm-wave signal, the transmission range is smaller compared to the Rayleigh model. Accordingly, the algebraic connectivity is less for the mm-wave transmission.

5.2. Multiple UAV simulation results

In this section, we provide the simulations results after solving Eq. (14) for multiple UAVs. Our goal is to find the optimal locations for the multiple UAVs that maximize the backhaul algebraic connectivity, subject to providing a certain SINR threshold for all the UEs.

Fig. 9 aims to show the performance of the proposed algorithm in the multiple UAV case. We consider the deployment of $K = 2$ UAVs aiming to serve $M = 8$ UEs. Fig. 9 shows that the proposed algorithm provides a better SCs connectivity, compared to the UAVs random positioning in both Rayleigh and mm-wave channels. Similar to the single-UAV case in Fig. 8, the mm-wave achieves a lower connectivity than the Rayleigh fading. Compared to the random positioning scheme, Fig. 9 shows that deploying 2

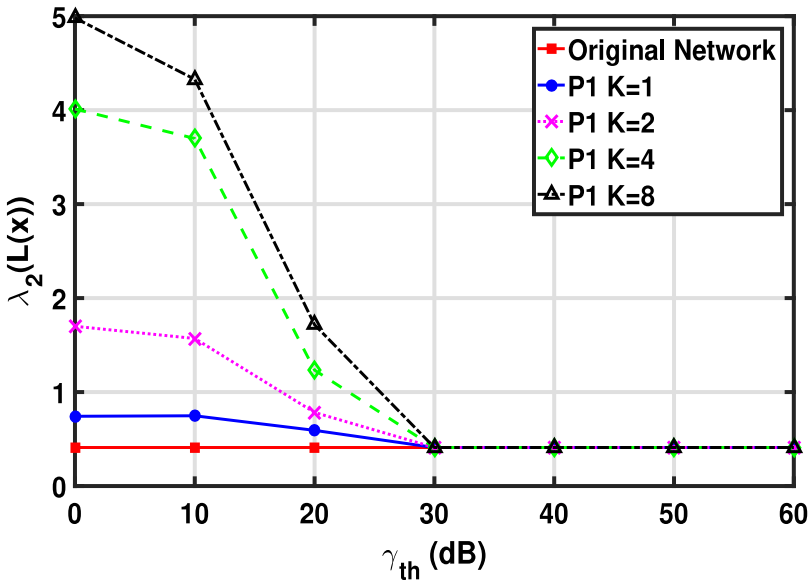

Fig. 10. The connectivity of the SCs versus the UEs γ_{th} for different number of UAVs.

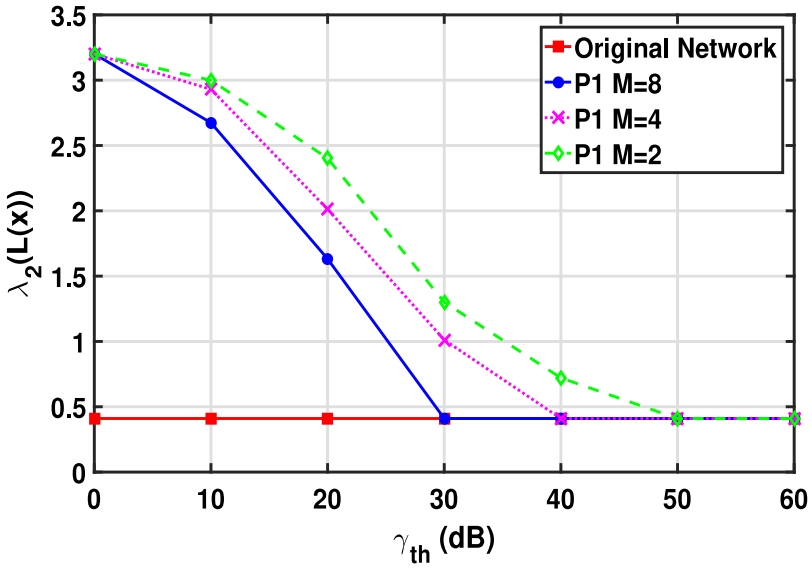

Fig. 11. The connectivity of the SCs versus the UEs γ_{th} for different number of UEs.

UAVs achieve performance gain of 100% for the Rayleigh channel and 80% for the mm-wave channel, at SINR threshold of 20 dB. Also, the achieved performance over the random positioning is almost 60% for both mm-wave and Rayleigh channel.

5.2.1. Impact of number of UAVs

In Fig. 10, the SCs connectivity is plotted against the UEs SINR threshold for different number of UAVs, $K = 1, 2, 4$ and 8, with mm-wave channel model. In this scenario, the connectivity of the SCs network grows with increasing the number of UAVs. For example, deploying $K = 4$ achieves a connectivity gain of almost 3 times (200% gain) the original network connectivity at SINR threshold of 20 dB.

5.2.2. Dependency on the number of UEs

Furthermore, we investigate the impact of the number of UEs, served by each UAV, by increasing the number of UEs, M, and keeping K fixed. In Fig. 11, the SCs connectivity is plotted versus the UEs SINR threshold γ_{th} at $K = 2$ UAVs. In this scenario, we notice a degradation in the algebraic connectivity as the number of UEs increases, which can be clarified as follows. Increasing the number of UEs forces more UAVs to come closer to them to achieve the required UEs SINR. Consequently, the UAVs moves away from the SCs which leads to lower algebraic connectivity for the SCs backhaul network.

6. Conclusion

The goal of this paper was to improve the integrated access and backhaul network through the optimal positioning of UAVs, and utilizing millimeter wave communication in the access network. In doing so, we have formulated a novel UAV positioning problem that aims to maximize the algebraic connectivity of the backhaul network, while guaranteeing a certain SINR (or QoS) on the served users. The considered optimization problem was relaxed to be an SDP one that can be solved numerically with reasonable complexity. The provided simulation results have shown

improvements that deploying one UAV can achieve enhancement of 80% to the backhaul algebraic connectivity, compared to the baseline random positioning schemes. Higher performance were indicated for the multiple UAVs. For example, at $K = 4$ UAVs, 200% improvement gain in the backhaul connectivity was achieved, compared to the random positioning scheme. The indicated connectivity enhancements are achieved, while guaranteeing the desired SINR at all the users over the mm-wave access network.

This work can be extended in the future by considering the *in-band* IAB scenario, in which both the access and backhaul networks operate on the same spectrum band. Formulating the backhaul connectivity maximization problem, while taking into consideration the interference impact from the access network, will be more challenging compared to the considered problem formulation in this paper. Finally, this work can be extended by considering optimal power allocation of the UAVs, as opposed to the equal power allocation policy considered in this work."

Declaration of competing interest

None.

References

[1] M.H. Tareque, M.S. Hossain, M. Atiquzzaman, On the routing in flying ad hoc networks, in: Federated Conference on Computer Science and Information Systems, FedCSIS, 2015, pp. 1–9.

[2] M. Berioli, A. Molinaro, S. Morosi, S. Scalise, Aerospace communications for emergency applications, Proc. IEEE 99 (11) (2011) 1922–1938.

[3] K. Miranda, A. Molinaro, T. Razafindralambo, A survey on rapidly deployable solutions for post-disaster networks, IEEE Commun. Mag. 54 (4) (2016) 117–123.

[4] V.S.H. Huynh, M. Radenkovic, A novel cross-layer framework for large scale emergency communications, in: International Wireless Communications and Mobile Computing Conference, IWCMC, 2017, pp. 2152–2157.

[5] S. Mignardi, R. Verdone, On the performance improvement of a cellular network supported by an unmanned aerial base station, in: International Teletraffic Congress, ITC 29, vol. 2, 2017, pp. 7–12.

[6] G.J. Lim, S. Kim, J. Cho, Y. Gong, A. Khodaei, Multi-uav pre-positioning and routing for power network damage assessment, IEEE Trans. Smart Grid (99) (2016) 1.

[7] C.X. Wang, A. Ghazal, B. Ai, Y. Liu, P. Fan, Channel measurements and models for high-speed train communication systems: A survey, IEEE Commun. Surv. Tutor. 18 (2) (2016) 974–987.

[8] L. Wei, R.Q. Hu, Y. Qian, G. Wu, Key elements to enable millimeter wave communications for 5g wireless systems, IEEE Wirel. Commun. 21 (6) (2014) 136–143.

[9] S. Geng, J. Kivinen, X. Zhao, P. Vainikainen, Millimeter-wave propagation channel characterization for short-range wireless communications, IEEE Trans. Veh. Technol. 58 (1) (2009) 3–13.

[10] W. Roh, J.Y. Seol, J. Park, B. Lee, J. Lee, Y. Kim, J. Cho, K. Cheun, F. Aryanfar, Millimeter-wave beamforming as an enabling technology for 5g cellular communications: theoretical feasibility and prototype results, IEEE Commun. Mag. 52 (2) (2014) 106–113.

[11] Z. Dejin, N. Yang, W. Liaoni, Z. Shenglu, A kind of moving net recovery technology for unmanned aerial vehicle, in: International Conference on Information and Communications Technologies, ICT, 2015, pp. 1–5.

[12] J. Dong, Q. Chen, Z. Niu, Random graph theory based connectivity analysis in wireless sensor networks with rayleigh fading channels, in: Asia-Pacific Conference on Communications, 2007, pp. 123–126.

[13] E. Yanmaz, Connectivity versus area coverage in unmanned aerial vehicle networks, in: IEEE International Conference on Communications, ICC, 2012, pp. 719–723.

[14] S. Rohde, C. Wietfeld, Interference aware positioning of aerial relays for cell overload and outage compensation, in: IEEE Vehicular Technology Conference, VTC, 2012, pp. 1–5.

[15] M. Mozaffari, W. Saad, M. Bennis, M. Debbah, Unmanned aerial vehicle with underlaid device-to-device communications: Performance and tradeoffs, IEEE Trans. Wirel. Commun. 15 (6) (2016) 3949–3963.

[16] E. Kalantari, M.Z. Shakir, H. Yanikomeroglu, A. Yongacoglu, Backhaul-aware robust 3d drone placement in 5g+ wireless networks, in: IEEE International Conference on Communications Workshops, ICC Workshops, 2017, pp. 109–114.

[17] M. Mozaffari, W. Saad, M. Bennis, M. Debbah, Drone small cells in the clouds: Design, deployment and performance analysis, in: IEEE Global Communications Conference, GLOBECOM, 2015, pp. 1–6..

[18] M.M. Azari, F. Rosas, K.C. Chen, S. Pollin, Optimal uav positioning for terrestrial-aerial communication in presence of fading, in: 2016 IEEE Global Communications Conference, GLOBECOM, 2016, pp. 1–7.

[19] X. Wu, C.X. Wang, J. Sun, J. Huang, R. Feng, Y. Yang, X. Ge, 60-ghz millimeter-wave channel measurements and modeling for indoor office environments, IEEE Trans. Antennas and Propagation 65 (4) (2017) 1912–1924.

[20] A. Thornburg, R.W. Heath, Capacity and coverage in clustered los mmwave ad hoc networks, in: IEEE Global Communications Conference, GLOBECOM, 2016, pp. 1–6.

[21] Z. Xiao, P. Xia, X. g. Xia, Enabling uav cellular with millimeter-wave communication: potentials and approaches, IEEE Commun. Mag. 54 (5) (2016) 66–73.

[22] L. Kong, L. Ye, F. Wu, M. Tao, G. Chen, A.V. Vasilakos, Autonomous relay for millimeter-wave wireless communications, IEEE J. Sel. Areas Commun. 35 (9) (2017) 2127–2136.

[23] J.L. Gross, J. Yellen, Handbook of Graph Theory, CRC press, Boca Raton.

[24] B. Slininger, Fiedlers Theory of Spectral Graph Partitioning, 2013.

[25] M.A. Abdel-Malek, A.S. Ibrahim, M. Mokhtar, Optimum UAV positioning for better coverage-connectivity tradeoff, in: IEEE International Symposium on Personal, Indoor, and Mobile Radio Communications, PIMRC, 2017, pp. 1–5.

[26] M. Mozaffari, W. Saad, M. Bennis, M. Debbah, Unmanned aerial vehicle with underlaid device-to-device communications: Performance and tradeoffs, IEEE Trans. Wirel. Commun. 15 (6) (2016) 3949–3963.

[27] M. Fiedler, Algebraic connectivity of graphs, Czechoslovak Math. J. 23 (2) (1973) 298–305.

[28] A. Ghosh, S. Boyd, Growing well-connected graphs, in: Proceedings of the 45th IEEE Conference on Decision and Control, 2006, pp. 6605–6611.

[29] Y.T. Hou, Y. Shi, H.D. Sherali, S.F. Midkiff, Prolonging sensor network lifetime with energy provisioning and relay node placement. in: IEEE Communications Society Conference on Sensor and Ad Hoc Communications and Networks, SECON, vol. 5, 2005, pp. 295–304.

[30] A.S. Ibrahim, K.G. Seddik, K.J.R. Liu, Connectivity-aware network maintenance and repair via relays deployment, IEEE Trans.n Wirel. Commun. 8 (1) (2009) 356–366.

[31] S. Boyd, L. Vandenberghe, Convex Optimization, Cambridge university press, 2004.

[32] M. Grant, S. Boyd, Y. Ye, Cvx: Matlab Software for Disciplined Convex Programming, 2008.

[33] K. Fujisawa, Y. Futakata, M. Kojima, S. Matsuyama, S. Nakamura, K. Nakata, M. Yamashita, Sdpa-m (semidefinite programming algorithm in matlab) user's manual-version 6.2, in: Research Reports on Mathematical and Computing Sciences, Series B: Operation Res., Dep. Math. and Computing Sci. Tokyo Institute of Technol., Japan, pp. 10.

[34] S. Sun, G.R. MacCartney, T.S. Rappaport, A novel millimeter-wave channel simulator and applications for 5g wireless communications, in: IEEE International Conference on Communications, ICC, 2017, pp. 1–7.

Mai A. Abdelmalek Currently a Ph.D. student in Electrical and Computer Engineering department (ECE) at Florida International University (FIU). She received the B.Sc degree (Hons.) in 2013 from the Communications and Electronic Department at Faculty of Engineering, Alexandria University, Egypt, and M.S in Wireless Technology from Nile University (NU), Egypt, in 2016. Worked as a research assistant at Wireless Intelligent Networks Center (WINC), NU. Worked as a research assistant at VirginiaTech-Middle East and North Africa (VT-MENA) for one year between August 2015 and August 2016.

Ahmed S. Ibrahim Dr. Ahmed S. Ibrahim is currently an assistant professor at the Electrical and Computer Engineering Department at Florida International University (FIU), Miami, FL, USA. He received the B.S. (with highest honors) and M.S. degrees in electronics and electrical communications engineering from Cairo University, Cairo, Egypt, in 2002 and 2004, respectively. He received the Ph.D. degree in electrical engineering from the University of Maryland, College Park, MD, USA, in 2009. Prior to joining FIU, Dr. Ibrahim was an assistant professor at Cairo University, wireless research scientist at Intel Corporation, and senior engineer at Interdigital Communications Inc. Dr. Ibrahim's research interests span various topics of next generation mobile communications and Internet of Things such as heterogeneous networks, drone-assisted millimeter wave communications, and vehicular networks.

Mohamed Mokhtar Mohamed Mokhtar is currently a senior 5G standards engineer at InterDigital, Inc. He received BSc degree in electronics and communications engineering from Alexandria University, Egypt, in 2008 and the MSc from Nile University, Egypt, in 2010. He earned his PhD degree in Electrical Engineering from University of Texas at Dallas, Richardson, TX, USA, in 2014. His research interests include cooperative communication and RF impairments equalization at the baseband.

Kemal Akkaya Dr. Kemal Akkaya is a full professor in the Department of Electrical and Computer Engineering at Florida International University. He received his PhD in Computer Science from University of Maryland Baltimore County in 2005 and joined the department of Computer Science at Southern Illinois University (SIU) as an assistant professor. Dr. Akkaya was an associate professor at SIU from 2011 to 2014. He was also a visiting professor at The George Washington University in Fall 2013. Dr. Akkaya leads the Advanced Wireless and Security Lab (ADWISE) in the ECE Dept. His current research interests include security and privacy, security and privacy, internet-of-things, and cyber-physical systems. Dr. Akkaya is a senior member of IEEE. He is the area editor of Elsevier Ad Hoc Network Journal and serves on the editorial board of IEEE Communication Surveys and Tutorials. He has served as the guest editor for Journal of High Speed Networks, Computer Communications Journal, Elsevier Ad Hoc Networks Journal and in the TPC of many leading wireless networking conferences including IEEE ICC, Globecom, LCN and WCNC. He has published over 150 papers in peer reviewed journal and conferences. He has received "Top Cited" article award from Elsevier in 2010.